

Reduction of Tin Oxide by Hydrogen Radicals

J. Wallinga,* W. M. Arnoldbik, A. M. Vredenberg, R. E. I. Schropp, and W. F. van der Weg

Interface Physics, Debye Institute, P.O. Box 80000, NL-3508 TA Utrecht, The Netherlands

Received: March 11, 1998; In Final Form: May 18, 1998

The effect of a reducing hydrogen ambient on textured tin oxide thin films on glass substrates has been investigated. Hydrogen treatments were done at 230 and 430 °C by hot wire (HW) and rf plasma-decomposed hydrogen with pure H₂ as source gas. By these treatments the possible reduction of the substrate during the deposition of *a*-Si:H for solar cells is simulated. Ion beam techniques revealed that the exposure to HW-decomposed H-radicals leads to the formation of a tin-rich surface layer of 40 nm in 1 min at both 230 and at 430 °C. The loss of oxygen is higher for the high-temperature treatment. The optical transmission at a wavelength of 800 nm is reduced from 80% to less than 20%, while the sheet resistance increases from 6 to 8 Ω/□. At both temperatures the reduction of fluorine-doped tin oxide (FTO) by a HW-treatment occurs faster than by rf plasma-decomposed H. The H radical concentration, which is higher for the HW-decomposed hydrogen as compared to rf plasma-decomposed hydrogen, is the most important factor in determining the rate of the reduction process. For short exposures to H radicals, the transparency and conductivity of the tin oxide may be completely restored by means of reoxidation in air at 400 °C. In contrast, prolonged exposure to H-radicals induces irreversible loss of transparency and conductivity, concomitant with formation of granule-like particles of metallic tin on the surface. A thin plasma-deposited *a*-Si:H-layer was found to effectively protect the FTO-layer against reduction due to HW-generated H-radicals.

1. Introduction

An amorphous silicon p⁺-i-n⁺ solar cell is usually deposited on a rough fluorine-doped tin oxide (FTO) front contact by plasma-enhanced chemical vapor deposition (PECVD).¹ During the initial stages of deposition of the hydrogenated amorphous silicon (*a*-Si:H), the FTO-layer is exposed to a silane plasma, which contains hydrogen radicals and ions, next to Si-containing species. From experiments where only H₂ was used as a process gas, and thus no layer is deposited, it is known that the hydrogen radicals and ions in the plasma interact with the FTO-layer² and cause a reduction of the tin oxide. This leads to a decrease in the transmission and an increase in the sheet resistance of the layers.

Schade et al.³ found that the effect of a hydrogen plasma exposure is influenced by an external dc-bias voltage. The dc-bias was interpreted to lead to a change of the ion flux. The results indicated that an additional bombardment with hydrogen ions during an H-radical treatment leads to enhanced reduction. In our opinion, however, applying an external bias, which leads to an increase of the deposition rate, will increase the radical flux.⁴ This implies that we consider it doubtful whether ions are the cause of the observed enhancement of the reduction of tin oxide.

In the range of substrate temperatures used for PECVD, i.e., from 100 to 250 °C, the loss of transmission and increase of sheet resistance become more prominent as temperature increases.^{3,5} Reoxidizing the samples is possible by a thermal annealing treatment in air at 400 °C for a few hours.² This treatment results in an almost complete recovery of the optoelectronic properties to the nontreated state. This restoration is certainly not obvious, since the temperature of the treatment

is well above the melt temperature of tin, i.e., 232 °C. Above the melt temperature, clustering of tin after the reduction of the tin oxide may occur, which causes irreversible changes to the tin oxide matrix.

Wanka et al.⁶ studied the interface between FTO and PECVD *a*-Si:H by XPS, using sputtering to obtain depth profiles. It was found that an SiO_x barrier layer with a deposition-rate-dependent thickness had formed at the interface during deposition. For a high deposition rate, the resulting SiO_x layer was thinner, indicating that shielding of the FTO-layer by the *a*-Si:H reduces the amount of reduction taking place.

The deposition of *a*-Si:H by hot wire chemical vapor deposition⁴ (HWCVD) usually takes place at substrate temperatures above 400 °C.⁷ This deposition method enables the preparation of device-quality films with a low hydrogen content,⁸ and the layers are reported to be less sensitive to the creation of metastable defects⁷ than those deposited by PECVD. Together with the high deposition rates of typically 1 nm/s,⁸ this makes the material very promising for application in *a*-Si:H solar cells. During the deposition of *a*-Si:H by HWCVD, the FTO-substrate is exposed to a mixture of silicon and hydrogen radicals, while no ions are involved.⁷ So far, it is not known whether the rate of the reduction of the FTO-layer by this method is comparable to what is observed with PECVD.

For tin-doped indium oxide layers (ITO) without surface texture, the effects of HW-decomposed and rf plasma-decomposed hydrogen have been compared by Lan and Kanicki.⁹ They showed that the effects of reduction of the indium oxide, i.e., a decrease in optical transmission, and an increase in sheet resistance are qualitatively the same for HW-decomposed and rf plasma-decomposed hydrogen treatments at 300 °C. However, because a textured layer is essential in a p⁺-i-n⁺ *a*-Si:H solar cell structure in order to increase the light absorption in a thin-film solar cell due to light scattering,¹⁰

* Corresponding author. E-mail: J.Wallinga@phys.uu.nl. FAX: +31 30 254 3165.

TABLE 1: Conditions Used for Tin Oxide Treatment^a

samples	treatment					
	LTHW1	HTHW1	LTPE10	HTPE10, HTPE4, HTPE1	deposition	
					HWSi	PESi ^b
time (min)	1	1	10	10, 4, 1	0.17	1
T_{treat} (°C)	230	430	230	430	430	230
HW or PE	HW	HW	PE	PE	HW	PE
H ₂ (sccm)	20	20	50	50		
SiH ₄ (sccm)					90	40
p (μ bar)	20	20	700	700	20	700

^a LT and HT denote low and high temperature. PE and HW denote plasma-decomposed and hot wire decomposed hydrogen treatment, respectively. ^b Sample PESi was treated with HW-hydrogen radicals at 430 °C for 1 min after deposition.

we study FTO-layers here. They have inherent surface texture, arising from the deposition of the layers on glass substrates by atmospheric pressure CVD.

The purpose of this study is to compare the degradation of APCVD tin oxide due to a treatment with hydrogen radicals from a hot wire and with a hydrogen plasma. Both the changes in chemical state and in surface morphology of textured SnO₂:F substrates were examined. Using ion beam techniques, depth profiles of the compositions have been obtained. Annealing treatments in air were performed to study the reoxidation behavior of the samples after the H treatments.

2. Experimental Section

For all experiments U-type SnO₂:F transparent conducting oxide layers on glass substrates from Asahi Glass Co. were used. The thickness of the APCVD-deposited polycrystalline FTO-layers is $\sim 1 \mu\text{m}$, and the height variations are around 50 nm over one crystal with a diameter of roughly 150 nm. The angle between the surface plane and the facets of the FTO-crystals, as determined by cross-sectional transmission electron microscopy (XTEM), is 33° on average but is distributed between 12 and 54°.

Both the plasma- and the HW-decomposed H-treatments of the FTO-substrates were performed in the PASTA¹¹ deposition system. The used hot-wire assembly consists of two tungsten wires with an effective length of 12 cm, situated 4 cm apart.¹² A wire temperature of 1850 °C was used for the HW decomposition of H₂. This wire temperature is well above the minimum temperature at which H₂ is effectively decomposed. All plasma-decomposed hydrogen treatments were performed at 13.56 MHz at a power of 3 W. The preparation conditions and sample denotations are summarized in Table 1.

To determine the influence of the substrate temperature on the reduction reaction, a low-temperature (LTHW1) treatment at 230 °C and a high-temperature (HTHW1) treatment at 430 °C were performed by hot wire decomposed hydrogen for 1 min. For comparison a plasma-decomposed hydrogen treatment was performed for 10 min at 230 °C (LTPE10) and 430 °C (HTPE10). Shorter plasma-decomposed H-treatments of 1 and 4 min were performed at 430 °C (HTPE1 and HTPE4). Reoxidation of these samples was performed in air at 400 °C for 120 min. In addition, two samples were made to study the influence of the deposition of $\sim 15 \text{ nm } a\text{-Si:H}$ on a tin oxide substrate. One layer was deposited by HWCVD at 430 °C (HWSi), and the other one was made by PECVD at 230 °C (PESi). The deposition times were 10 s and 1 min, respectively. After deposition the low-temperature PECVD-sample was heated to 430 °C and a 1 min HW-decomposed hydrogen treatment was performed.

The chemical binding state of tin and oxygen in the first $\sim 10 \text{ nm}$ at the surface of an FTO-layer before treatment and of sample HTHW1 were determined by X-ray photoelectron spectroscopy (XPS) with the K α X-rays obtained from electron bombardment of an Al-target. The XPS data were taken ex situ.

The surface morphology of FTO-layers before treatment, the H-treated samples, and the reoxidized samples was examined by scanning electron microscopy (SEM), using a Philips XL30-FEG electron microscope. Element analysis was performed on these samples, by energy dispersive X-ray (EDX) analyses of the Sn L-lines and the O K-lines, using electron energies of 7 keV.

The depth profile of tin upon reduction due to a H-treatment was studied by means of Rutherford backscattering spectrometry (RBS). Elastic recoil detection (ERD) was used to determine the oxygen concentration profiles. The analysis of the ion spectroscopy measurements is complicated by the native surface texture of the FTO-layers and the change of morphology upon treatment. Because of the spot sizes of at least $1 \times 1 \text{ mm}^2$, the obtained signals are an average over the various facet angle orientations at the sample surface.

For the RBS-analysis a 1 MeV He⁺ ion beam produced by a 3 MeV single-ended Van de Graaff accelerator was used. The angle between the beam and the sample surface amounted to 90°. Scattered particles were detected under an angle θ of 170°, relative to the beam, as indicated in the inset of Figure 4a. The RBS-spectra were analyzed using the computer code RUMP.¹³ Six curves have been calculated for different facet angles of plus and minus 23, 33, and 43° for all samples, thus mimicking the surface roughness as known from XTEM. The presented simulations are the average of these six curves and thus account for the surface roughness of the FTO-layers. From the height of the tin profiles of the treated samples compared to that of the nontreated ones, we extracted the relative variation in the tin content.

The change in oxygen concentration of the top layer is determined by elastic recoil detection (ERD).¹⁴ A 45 MeV ⁶³Cu-beam produced by a 6.5 MeV tandem Van de Graaff accelerator was used. The angle α of the incoming beam with the surface was varied between 17.5 and 24.5°, and the recoil angle ϕ was 30–37°. A 12 μm Mylar foil in front of the stop-detector was used to obtain background-free ERD signals. Because of the small angles involved in these measurements, the influence of surface roughness was expected to be large.¹⁵ However, in comparing the ERD-signal of a rough and a polished FTO-layer, we found relatively small changes. Moreover, because the results for the different measurement configurations are consistent, qualitative comparison of the results is possible. We present here data for $\alpha = 17.5^\circ$ and $\phi = 30^\circ$. The measurement configuration is schematically depicted in the inset of Figure 6.

The influence of the tin oxide reduction on the transmission of the FTO-layers was measured using a Perkin-Elmer Lambda 2S spectrophotometer. We quote here the transmission at a wavelength of 800 nm. The sheet resistance of the FTO-layers is determined using a four-point measurement.

3. Results

3.1. HW-Decomposed Hydrogen Radicals. Figure 1 shows the measured XPS-data of the SnO₂:F sample before any treatment and of the HTHW1-sample. Before treatment no metallic tin is detected; tin is only present in the SnO₂-configuration.¹⁶ However, the HW hydrogen radical treated film

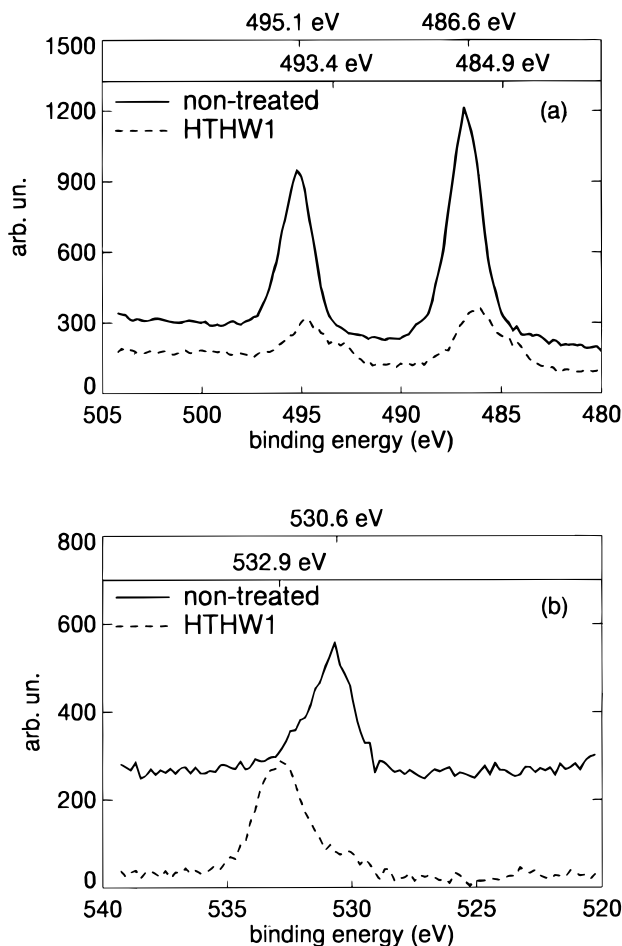


Figure 1. XPS spectra of (a) tin and (b) oxygen. The peaks at a binding energy of 486.6 and 495.1 eV for tin 3d_{5/2} and 3d_{3/2} relate to SnO₂. The metallic tin peaks are 3d_{5/2} at 484.9 eV and 3d_{3/2} at 493.4 eV.¹⁶ The 1s oxygen binding energy of SnO₂ is found at 530.6 eV, while the binding energy of 532.9 eV relates to the 1s oxygen binding energy of SiO₂.

shows tin peaks at the binding energy corresponding to metallic tin. The corresponding peak heights are comparable in size to the peaks due to binding of Sn⁴⁺ in SnO₂, even though some surface oxidation could have taken place during transportation of the samples in air. The lower intensity of both peaks with respect to the sample before treatment is due to the presence of silicon at the surface of the sample. This is caused by a small release of silicon from the walls of the reactor while the sample is heated and treated. The only oxygen-related peak in the spectrum of the sample before treatment is due to oxygen in SnO₂. In the oxygen signal of sample HTHW1, no signal due to SnO₂ is found. It shows one distinct peak in agreement with SiO₂. It is thus clear that HW-decomposed hydrogen radicals cause a reduction reaction at the surface of a tin oxide layer.

The SEM-image for sample HTHW1 shows an onset of sphere formation, as can be seen from the appearance of a few 'white' particles in Figure 2b. The surface of the nontreated sample is shown in Figure 2a. In addition to the formation of particles at the surface, also the morphology has changed from the polycrystalline structure to a more rounded, and larger, structure upon the treatment with HW-decomposed hydrogen radicals. It is confirmed that the tin particles that formed on sample HTHW1 do not disappear upon annealing. The surface morphology for sample LTHW1 is depicted in Figure 2c and is comparable to that for sample HTHW1. At the lower

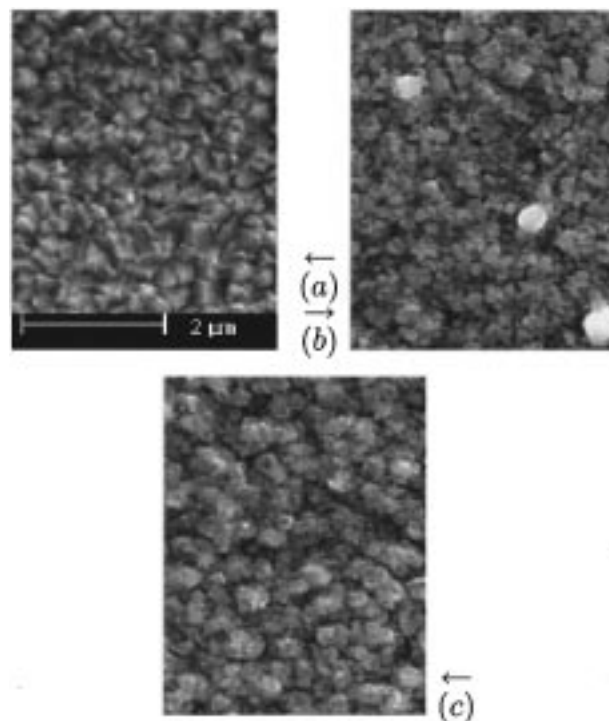


Figure 2. SEM-pictures of (a) tin oxide before treatment, (b) HTHW1, (c) LTHW1. Magnification for all pictures as indicated in (a).

temperature, there was no sphere formation, indicating that the reduction at lower temperatures is less severe.

In Figure 3a the optical transmission at a wavelength of 800 nm is plotted, both after the different H-treatments and after the subsequent reoxidation in air. For the 1 min treatments with HW-decomposed hydrogen, both at low and high temperature, the decrease in transmission is fully reversible.

Upon hydrogen radical treatment the sheet resistance of the samples increases, as is shown in Figure 3b together with the effect of subsequent heat treatments at 400 °C in air. The starting value was 6 Ω/□. After the low and high temperature HW-decomposed hydrogen treatment, the resistance increased slightly to 8 Ω/□. No significant change was observed upon reoxidation.

The RBS-spectra of the HW-treated samples are depicted in Figure 4a,b together with the simulations. From the tin signal in this measurement, we find that a surface layer of 40 nm has changed in composition from SnO₂ to SnO for the LTHW1 sample and to SnO_{0.6} for the HTHW1 sample. Below this surface layer another layer of 55 nm is present, which contains slightly more tin than the bulk SnO₂. Thus RBS-measurements show relatively more tin for the sample treated at high temperature than for that treated at low temperature. For both samples the reoxidation is complete after the heat treatment in air at 400 °C, as is also shown in Figure 4a,b.

The results of the ERD-measurements are shown in Figure 5. The surface morphology inhibits a quantitative interpretation of the data. Owing to the changes in surface morphology upon the hydrogen radical treatments, care should also be taken in the qualitative comparison of the data. Nevertheless, for the LTHW1 and HTHW1 samples we observe that the oxygen content at the surface has dropped, over a depth range in agreement with the RBS-data. The largest change is observed for the high temperature sample. From Figure 5 it is seen that the oxygen concentration in the reoxidized samples is completely restored.

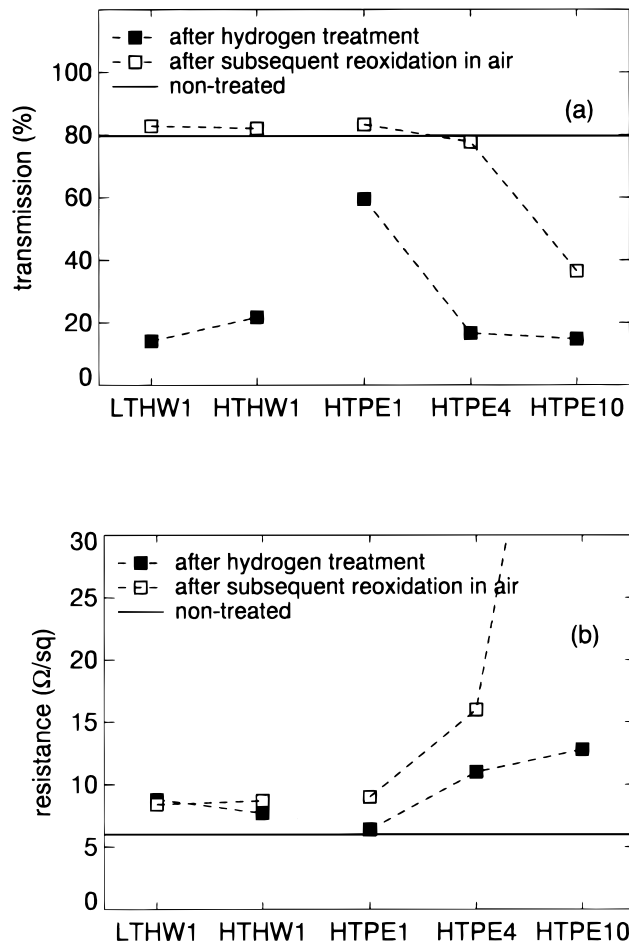


Figure 3. (a) Transmission and (b) sheet resistance after H-treatment and after subsequent heat treatment in air at 400 °C for 120 min.

No changes in conductivity and transmission were observed for a sample that was only heated to 430 °C in a vacuum.

3.2. Plasma-Decomposed Hydrogen Radicals and Ions.

The effect of plasma-decomposed H-radicals and ions on the surface morphology of textured tin oxide after a 1 min treatment at 430 °C, sample HTPE1, is shown in Figure 7a. The rounded surface structure of sample HTPE1 is changed into a polycrystalline morphology after reoxidation in air at 400 °C for 120 min as is shown in Figure 7b.

From the SEM-image in Figure 7c, it is clear that the exposure to plasma-decomposed hydrogen radicals and ions at 430 °C leads to the formation of spheres on the sample surface after 4 min (HTPE4). This effect increases, and after 10 min tile-like structures have grown to a size of 2 μm (HTPE10), as is shown in Figure 7d. This formation of surface spheres is similar to what is reported for ITO.^{9,17} Using EDX we found that the spheres consist of tin; the oxygen concentration in the large spheres on the sample surface was below the detection limit of 1%.

The transmission of sample HTPE1 is fully restored upon the heat treatment, as is shown in Figure 3a. However, the transmission of the sample HTPE10, which is comparable to HTPE1 after the hydrogen treatment, is still below 40% after the anneal in air. The onset of an irreversible change in transmission is seen in the HTPE4 sample, where the transmission is slightly lower after the heat treatment.

The HTPE1 sample showed no increase in resistance upon treatment. However, the value increased after the heat treatment in air, which restored the transmission. For the HTPE4 and

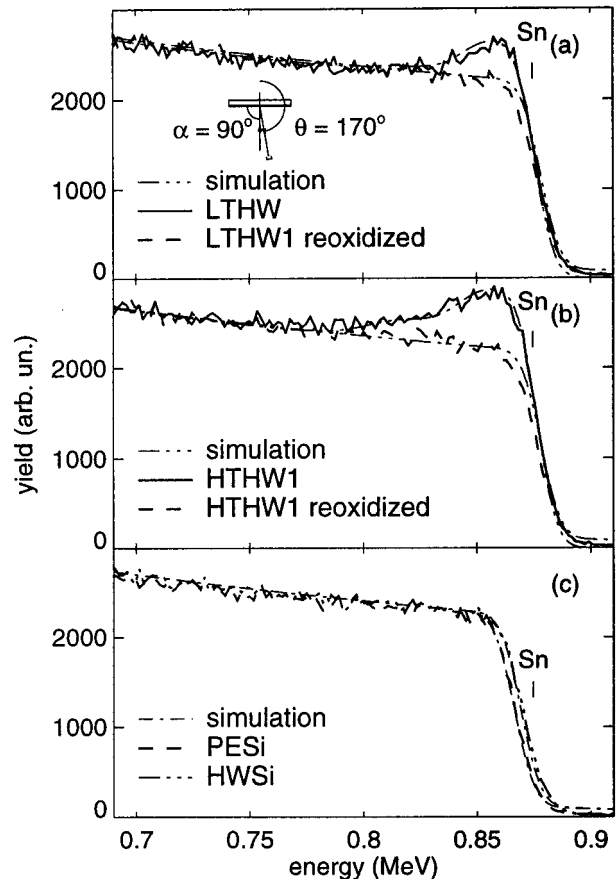


Figure 4. RBS spectra for samples (a) LTHW1, (b) HTHW1 after H-treatment and after reoxidation, (c) PESi and HWSi. In the plots the surface energy of Sn is indicated. In the inset of (a) the measurement configuration is depicted.

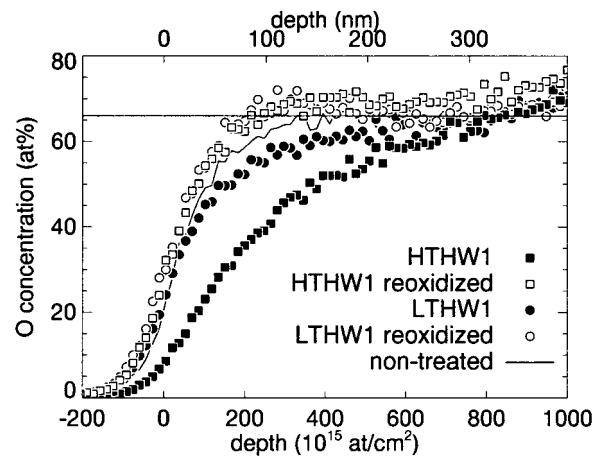


Figure 5. Oxygen depth profiles as measured by ERD before treatment, H-treated, and annealed samples. The line at 66.7 at% O denotes stoichiometric SnO₂.

HTPE10 samples the resistance increased to 10–12 Ω/□. After the heat treatments in air the resistance of these samples rose to values of 16 and 60 Ω/□, respectively.

The LTPE10 sample did not show any changes in transmission, sheet resistance, or tin-profile after the plasma-decomposed hydrogen treatment.

3.3. Deposition of Thin *a*-Si:H-Layers. As is shown in Figure 4c, the RBS-spectra from sample HWSi and sample PESi are comparable, apart from a slightly thicker *a*-Si:H-layer in case of the PECVD-sample. The thicknesses of the *a*-Si:H-layer derived from these measurements are 17 and 12 nm for

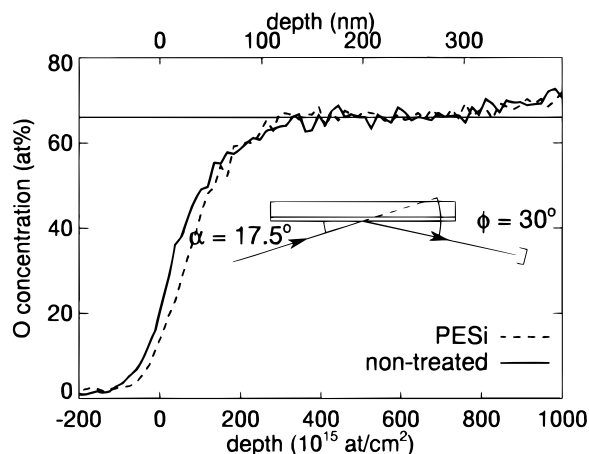


Figure 6. Oxygen depth profiles as measured by ERD without deposition (nontreated) and after deposition of a thin PECVD-layer with subsequent HW-decomposed H-treatment (HWSi). The inset shows the measurement configuration.

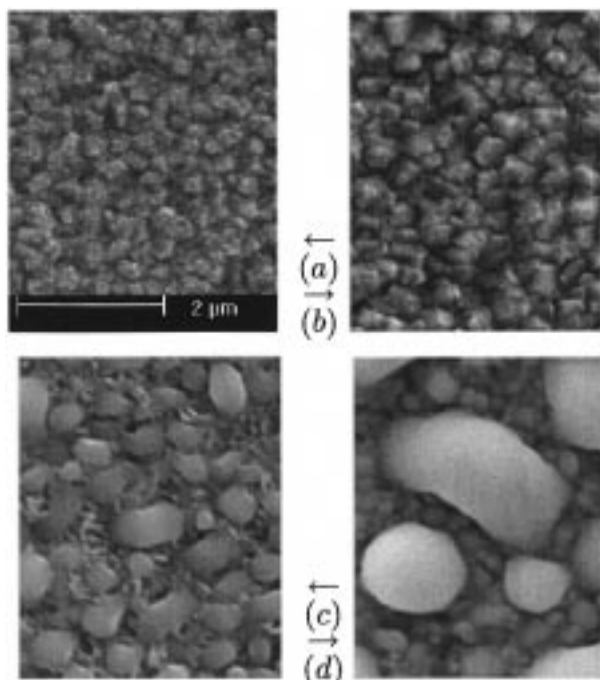


Figure 7. SEM-pictures of (a) HTPE1, (b) HTPE1 after reoxidation, (c) HTPE4, (d) HTPE10. Magnification for all pictures as indicated in (a).

the PECVD and HWCVD *a*-Si:H-layers, respectively. The amount of tin in the Si-layer is below the detection limit of 5 at. %.

The ERD oxygen profile of the 17 nm PECVD-sample in Figure 6 does not show any oxygen in the top ~ 13 nm of the *a*-Si:H-layer. From these measurements we cannot exclude the formation of a thin silicon oxide layer at the interface between the *a*-Si:H and the FTO.

4. Discussion

4.1. Radical Fluxes. The deposition rate of PECVD *a*-Si:H-layers is mainly related to the flux of Si-containing radicals to the surface.¹⁸ The same holds for deposition of *a*-Si:H by HWCVD. Because the deposition rate for HWCVD is typically five times higher than for PECVD, we infer that also the radical flux is larger. When only H₂ is used as source gas, we assume that also the flux of hydrogen radicals to the

surface is higher in case of HW as compared to a plasma. It is therefore expected that radical-related effects on the tin oxide layer can only be meaningfully compared for plasma-treated samples with a treatment time that is longer than for HW-decomposed hydrogen treated samples.

During an actual HWCVD deposition, when pure SiH₄ is fed into the process chamber, the hydrogen-radical concentration typically is a factor of 10 lower than in the case of pure hydrogen.¹⁹ The effect of hydrogen radicals due to decomposition of SiH₄ will thus be much less than that due to decomposition of H₂ for the same duration. Although a lower radical concentration with the use of SiH₄ instead of H₂ is also expected in the case of PECVD, we have not found evidence for this.

Apart from this, upon deposition the substrate is only gradually shielded from the influence of hydrogen radicals and ions. Recent measurements in our group²⁰ showed that HW-decomposed hydrogen radical treatments affect the hydrogen concentration in *a*-Si:H-layers up to a depth of 200 nm.

4.2. Reduction Behavior. Besides the measurements presented in the previous sections, there is also a clearly visible difference between the samples. The samples that show darkening after the hydrogen treatment become transparent upon a heat treatment in air. The ones that show whitening after H-treatment retain a low transmission after the heat treatment. The whitening results from strong light scattering from the surface, which is in agreement with the morphology observed by SEM.

At a temperature of 230 °C, the difference between the plasma- and HW-decomposed H-treatments appears to be large. Sample LTPE10, exposed to 10 min plasma-decomposed H, does not show any reduction. In contrast to this, the sample that was treated for 1 min by HW-decomposed hydrogen at approximately the same temperature shows strong reduction of the surface tin oxide layer. This is thought to be mainly caused by small variations in temperature between the PECVD- and HWCVD-treatments, as a result of differences in substrate heating. The absence of reduction for sample LTPE10 at 230 °C is different from what is observed by Schade et al. at temperatures below 250 °C.³ This might indicate the superior quality of the FTO used in our experiments. At a higher temperatures, i.e., above the melt temperature of tin, the stability in plasma-decomposed hydrogen is lost and we observe a strong temperature dependence of the reduction, similar to Schade et al.³

We have shown that at 430 °C, up to a threshold that is between 1 and 4 min for plasma-decomposed H and is slightly less than 1 min for HW-decomposed hydrogen, the damage done to the FTO-substrates by these treatments is almost fully reversible. Even at temperatures well above the melt temperature of tin, the decrease in optical transmission due to a hydrogen treatment can be recovered by oxidation in air at 400 °C for 2 h. It is clear from Figure 7b that the polycrystalline nature of the tin oxide has to a large extent been recovered owing to the annealing. The time for an HW H-treatment to form Sn surface spheres is one to four times shorter than for a hydrogen plasma. This is in agreement with the ratio of the hydrogen radical fluxes of the two deposition methods.

After prolonged treatment with plasma-decomposed hydrogen radicals and ions, particles started to form at the tin oxide surface. It is confirmed that these are tin droplets. This nucleation into droplets of elemental tin at the surface of the reduced tin oxide leads to the continued renewed exposure of not-fully reduced tin oxide to hydrogen radicals. Consequently a large loss of oxygen from the sample is possible. Once tin

particles have formed, the reduction process is not reversible by reoxidation at 400 °C in air anymore.

XTEM on an FTO-layer with an HWCVD *a*-Si:H-layer deposited on top at a substrate temperature of 440 °C previously showed that an interface layer with a thickness of 100 nm⁴ has formed between the tin oxide and the *a*-Si:H, which indicates a reduction of the top of the tin oxide.

In contrast to this, after the deposition of a 10 nm PECVD *a*-Si:H-layer at 230 °C and subsequent HW-decomposed H-treatment, no reduction of the tin oxide and no oxygen in the upper region of the *a*-Si:H-layer are detected. We attribute this stability against reduction to the formation of a thin silicon oxide layer at the *a*-Si:H-FTO-interface. Because it is known that 10 nm *a*-Si:H does not form a diffusion barrier for H-radicals, it is expected that during H-radical treatment at first a thin silicon oxide layer is formed, which subsequently acts as a barrier layer. It even is possible that such a layer will form at the FTO-*a*-Si:H interface upon deposition of the *a*-Si:H, similar to what was found by Wanka et al.⁶ According to a study by Lan and Kanicki,⁹ a SiO₂ barrier layer, which prevents a metal oxide surface from reduction, can also be deposited by PECVD. Solar cells with a 5 nm SiO barrier on top of the TCO have been reported by de Nijs et al.²¹ We infer this could also be a suitable method for depositing HWCVD *a*-Si:H on FTO.

5. Conclusion

At 430 °C HW-created hydrogen radicals lead to the reduction of textured tin oxide and the formation of tin particles at the surface within 1 min. This is one to four times faster than with plasma-decomposed hydrogen at the same temperature. At lower temperature, 230 °C, the stability of the FTO under plasma-decomposed hydrogen is lost for HW-decomposed hydrogen. Nevertheless at the lower temperature less reduction is found, indicating a strong temperature dependence. The chemical reduction reaction leads to a less transparent film with a higher sheet resistance. The comparison between the reduction by HW- and plasma-decomposed hydrogen shows that the combined exposure to ions and radicals in the hydrogen plasma does not induce different processes at the tin oxide surface than the exposure to HW-decomposed hydrogen radicals alone. When elemental tin aggregates into tin particles after prolonged reduction, oxidation in air no longer leads to recovery of the original optoelectronic properties. Before the onset of particle formation these properties can be recovered completely, including the polycrystalline nature of the film. A barrier layer of silicon oxide prevents the reduction and was formed by depositing a thin low-temperature plasma *a*-Si:H-layer, followed by a HW-decomposed hydrogen treatment at high temperature. The deposition of a PECVD SiO₂-layer on the FTO substrate before deposition of HW *a*-Si:H will be investigated in the future.

Acknowledgment. This work was financially supported by the Netherlands Agency for Energy and the Environment (NOVEM). We gratefully acknowledge C. H. M. van der Werf for the preparation of the samples, E. M. B. Heller for the XPS-measurements, and E. A. G. Hamers for the extensive discussions. We thank Asahi Glass Co. for the supply of tin oxide substrates.

References and Notes

- (1) Crandall, R.; Luft, W. *Prog. Photovoltaics* **1995**, *3*, 315.
- (2) Major, S.; Kumar, S.; Bhatnagar, M.; Chopra, K. L. *Appl. Phys. Lett.* **1986**, *49*, 394.
- (3) Schade, H.; Smith, Z. E.; Thomas, J. H., III; Catalano, A. *Thin Solid Films* **1984**, *117*, 149.
- (4) Wallinga, J.; Knoesen, D.; Hamers, E. A. G.; van Sark, W. G. J. H. M.; van der Weg, W. F.; Schropp, R. E. I. Plasma induced changes to TCO/*a*-Si:H interfaces. In *Amorphous Silicon Technology—1996*; Hack, M., Schiff, E. A., Wagner, S., Schropp, R., Matsuda, A., Eds.; Materials Research Society: Pittsburgh, PA, 1996.
- (5) Shiratsuchi, R.; Hirata, M.; Misonou, M.; Kawahara, H., Performance of *a*-Si:H solar cells with H₂ plasma pretreated SnO₂:F films. In *Technical Digest of the International PVSEC-3*; Publication Office PVSEC: Tokyo, 1987; pp 619–622.
- (6) Wanka, H. N.; Schubert, M. B.; Lotter, E., Investigation of TCO/p-interface and surface morphology of *a*-Si:H solar cells by in-situ ellipsometry. In *First WCPEC, Hawaii*; IEEE: Piscataway, NJ, 1994; pp 516–519.
- (7) Papadopoulos, P.; Scholz, A.; Bauer, S.; Schröder, B.; Oechsner, H. *J. Non-Cryst. Solids* **1993**, *164–166*, 87.
- (8) Mahan, A. H.; Carapella, J.; Nelson, B. P.; Crandall, R. S.; Balberg, I. *J. Appl. Phys.* **1991**, *69*, 6728.
- (9) Lan, J.-H.; Kanicki, J. *Thin Solid Films* **1997**, *304*, 123.
- (10) Yablonoitch, E.; Cody, G. D. *IEEE Trans. Electron Devices* **1982**, *29*, 300.
- (11) Madan, A.; Rava, P.; Schropp, R. E. I.; von Roedern, B. *Appl. Surf. Sci.* **1993**, *70–71*, 716.
- (12) Schropp, R. E. I.; Feenstra, K. F.; Molenbroek, E. C.; Meiling, H.; Rath, J. K. *Philos. Mag. B* **1997**, *76*, 309.
- (13) Doolittle, L. R. *Nucl. Instrum. Methods Phys. Res. B* **1986**, *15*, 227.
- (14) Arnoldbik, W. M.; Habraken, F. H. P. M. *Rep. Prog. Phys.* **1993**, *56*, 859.
- (15) Itoh, Y.; Maeda, T.; Nakajima, T.; Kitamura, A.; Ogiwara, N.; Saidoh, M. *Nucl. Instrum. Methods Phys. Res. B* **1996**, *117*, 161.
- (16) Chastrain, J., Ed. *Handbook of X-ray photoelectron spectroscopy*; Perkin-Elmer: Eden Prairie, MN, 1992.
- (17) Kuboi, O. *Jpn. J. Appl. Phys.* **1981**, *20*, L783.
- (18) Hamers, E. A. G.; van Sark, W. G. J. H. M.; Bezemer, J.; van der Weg, W. F.; Goedheer, W. J. Ion energy distributions in silane-hydrogen plasmas. In *Amorphous Silicon Technology—1996*; Hack, M., Schiff, E. A., Wagner, S., Schropp, R., Matsuda, A., Eds.; Materials Research Society: Pittsburgh, PA, 1996.
- (19) Tsuji, N.; Akiyama, T.; Komiyama, H. *J. Non-Cryst. Solids* **1996**, *198–200*, 1034.
- (20) Feenstra, K. F. Private communication.
- (21) de Nijs, M. M.; Carvalho, C.; Santos, M.; Martins, R. *Appl. Surf. Sci.* **1991**, *52*, 339.